JOURNAL OF SOLID STATE CHEMISTRY **126,** 235–241 (1996)
ARTICLE NO. 0334

Role of Tetravalent Ion in Metal–Insulator Transition in $(La_{0.1}Ca_{0.9})(Mn_{1-x}Ti_x)O_3$

Hideki Taguchi,* Masanori Sonoda, and Mahiko Nagao

Research Laboratory for Surface Science, Faculty of Science, Okayama University, Okayama 700, Japan

and

Hiroyasu Kido

Osaka Municipal Technical, Jyoto-Ku, Osaka 536, Japan

Received August 7, 1995; in revised form July 17, 1996; accepted July 18, 1996

Perovskite-type $(La_{0.1}Ca_{0.9})(Mn_{1-x}Ti_x)O_3$ ($0 \leq \times \leq 0.9$) has the orthorhombic $GdFeO_3$-type structure with the space group *Pnma*. With increasing *x*, the average (Mn, Ti)–O distance increases linearly and the average angles for (Mn, Ti)–O–(Mn, Ti) decrease slightly. The electrical resistivity (ρ) of all manganates was measured in the temperature range from 10 to 953 K. All manganates are *n*-type semiconductors at low temperature. At high temperature, the manganates exhibit a metal–insulator transition in the range $0 \leq x \leq 0.3$. $d\rho/dT$ in the metallic region depends on the composition. From these results, it is considered that the Ti^{4+} ion makes the cation–anion–cation overlap integrals (Δ^{π}_{cac} and Δ^{σ}_{cac}) weaken.

INTRODUCTION

$(Ln_{1-x}Ca_x)MnO_3$ (*Ln* = La, Nd, Gd, Tb, Ho, and Y) has the orthorhombic perovskite-type structure, and exhibits *n*-type semiconductor behavior at low temperature (1–5). At low temperature, the electrical resistivity (ρ) of these manganates follows Mott's $T^{-1/4}$ law, indicating the possible occurrence of variable range hopping of electrons due to Anderson localization (6). At high temperature, the electrical resistivity of these manganates has a positive temperature coefficient (α), and the metal–insulator transition occurs without any crystallographic change. From the magnetic measurements of these manganates, the spin state of the Mn^{3+} ion changes from low to high at the metal–insulator transition temperature (T_t) (1–3).

T_t of $(Ln_{1-x}Ca_x)MnO_3$ decreases with increasing *x*. At a particular value of *x*, T_t increases with increasing ionic radius of the rare earth ion (7). In the metallic region, with increasing *x*, the temperature coefficient (α) of the electrical resistivity monotonically increases with little difference among La^{3+}, Nd^{3+}, and Gd^{3+} ions (7). The increase in $d\rho/dT$ is explained by both the decrease in the Mn–O distance and the number of 3*d* electrons that exist in the Mn^{3+} ion with the high-spin state. From the increase in $d\rho/dT$ in $(Nd_{0.1}Ca_{0.9})(Mn_{1-x}Al_x)O_3$, the number of 3*d* electrons in the conduction band plays an important role in controlling $d\rho/dT$ of these manganates (8).

Although the role of a trivalent ion and the *Ln* ion in the metal–insulator transition in $(Ln_{1-x}Ca_x)MnO_3$ has been investigated, the role of a tetravalent ion has not been reported. In the present study, we tried to synthesize a $(La_{0.1}Ca_{0.9})(Mn_{1-x}Ti_x)O_3$ ($0 \leq x \leq 0.9$) sample. This sample is expressed as $(La^{3+}_{0.1}Ca^{2+}_{0.9})[Mn^{3+}_{0.1}(Mn^{4+}_{0.9-x}Ti^{4+}_x)]O_3$. As the Ti^{4+} ion has no 3*d* electrons, it is expected that the total number of 3*d* electrons will decrease linearly with increasing *x*. From the relationship between the average (Mn, Ti)–O distance and the electrical properties, we will make clear the role of the tetravalent ion in the metal–insulator transition.

EXPERIMENTAL

$(La_{0.1}Ca_{0.9})(Mn_{1-x}Ti_x)O_3$ ($0 \leq x \leq 0.9$) samples were prepared by a standard ceramic technique. Dried La_2O_3, $CaCO_3$, MnO_2, and TiO_2 powders were weighed in the appropriate proportions and milled for a few hours with acetone. After the mixed powders were dried at 373 K, they were calcined at 1173 K for 12 hr in air, then fired at 1573 K for 24 hr under a flow of pure oxygen gas. In order to measure the electrical resistivities of the samples, the powders were pressed into a pellet form under a pressure

* To whom all correspondence should be addressed.

0022-4596/96 $18.00

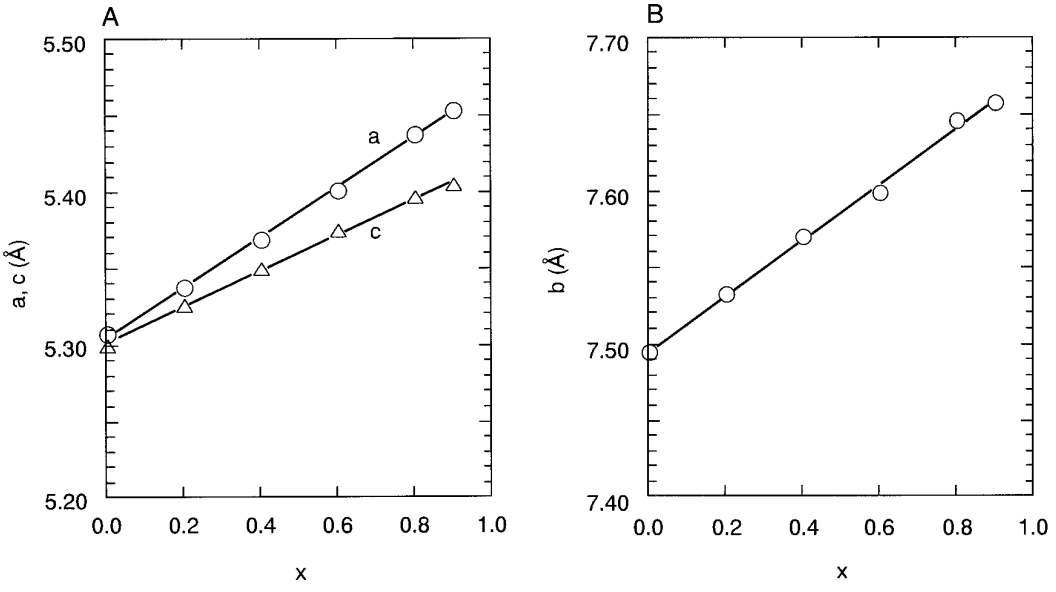

FIG 1. Cell constants (a, b, and c) vs composition (x) for the system $(La_{0.1}Ca_{0.9})(Mn_{1-x}Ti_x)O_3$.

of 50 MPa, and the pellet was sintered at 1573 K for 12 hr under the flow of pure oxygen gas. The samples obtained in this manner were annealed at 973 K for 24 hr under the flow of pure oxygen gas.

The phases of the samples were identified by X-ray powder diffraction with monochromatic Cu$K\alpha$ radiation. The cell constants of the samples were determined from high-angle reflections with Si as an external standard. The structure refinement was carried out by the Rietveld analysis of the X-ray powder diffraction data with the "RIETAN" program written by Izumi (9). X-ray diffraction data were collected by step scanning over an angular range of $20° \leq 2\theta \leq 100°$ in increments of 0.02° (2θ) with monochromatic Cu$K\alpha$ radiation. The electrical resistivity of the samples was measured by a standard four-electrode technique in the temperature range 10–953 K.

The magnetic susceptibility of $(La_{0.1}Ca_{0.9})(Mn_{0.8}Ti_{0.2})O_3$ ($x = 0.2$) was measured by a magnetic torsion balance in the temperature range 303–713 K.

RESULTS AND DISCUSSION

X-ray powder diffraction patterns of $(La_{0.1}Ca_{0.9})(Mn_{1-x}Ti_x)O_3$ ($0 \leq x \leq 0.9$) were completely indexed as the orthorhombic perovskite-type ($GdFeO_3$-type) structure. Figure 1 shows the relationship between the cell constants (a, b, and c axes) and the composition. The cell constants increase linearly with increasing x. Figure 2 shows the relationship between the cell volume and the composition. The cell volume increases linearly with increasing x. These results indicate that the Ti^{4+} ion was substituted for the Mn^{4+} ion in $(La_{0.1}Ca_{0.9})(Mn_{1-x}Ti_x)O_3$. The ionic radius of the Mn^{4+} ion and the Ti^{4+} ion with a coordination number (CN) of 6 are 0.54 and 0.605 Å, respectively (10). Therefore, variation in Figs. 1 and 2 is explained by the difference in the ionic radius between the Mn^{4+} and Ti^{4+} ions.

The structure refinement of $(La_{0.1}Ca_{0.9})(Mn_{1-x}Ti_x)O_3$ was carried out by the Rietveld analysis of X-ray powder diffraction data. $(La_{0.1}Ca_{0.9})(Mn_{1-x}Ti_x)O_3$ has an orthorhombic $GdFeO_3$-type structure with the space group $Pnma$ (11). In the present study, isotropic thermal parameters (B) for La, Ca, Mn, Ti, O(1), and O(2) ions were fixed

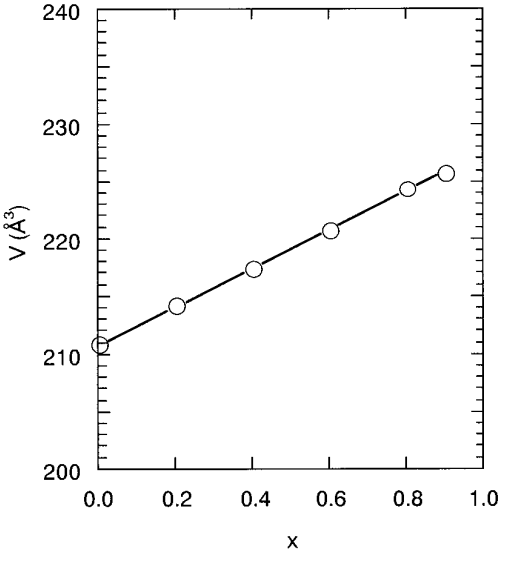

FIG 2. Cell volume (V) vs composition (x) for the system $(La_{0.1}Ca_{0.9})(Mn_{1-x}Ti_x)O_3$.

TABLE 1
Refined Structure Parameters for $(La_{0.1}Ca_{0.9})(Mn_{1-x}Ti_x)O_3$

$x = 0.0$	$a = 5.3072(2)$ Å	$b = 7.4945(2)$ Å	$c = 5.3006(2)$ Å		
	$R_{WP} = 12.86\%$	$R_p = 8.84\%$	$R_I = 3.43\%$		$R_F = 3.33\%$
Atom	Position	x	y	z	B
La, Ca	4(c)	0.027(1)	0.25	−0.006(2)	0.3
Mn	4(b)	0	0	0.5	0.3
O(1)	4(c)	0.491(3)	0.25	0.068(6)	0.3
O(2)	8(d)	0.286(4)	0.030(3)	−0.284(4)	0.3
$x = 0.2$	$a = 5.3370(2)$ Å	$b = 7.5322(3)$ Å	$c = 5.3267(2)$ Å		
	$R_{WP} = 12.70\%$	$R_p = 8.67\%$	$R_I = 3.02\%$		$R_F = 2.59\%$
Atom	Position	x	y	z	B
La, Ca	4(c)	0.026(1)	0.25	−0.005(3)	0.3
Mn, Ti	4(b)	0	0	0.5	0.3
O(1)	4(c)	0.490(3)	0.25	0.073(7)	0.3
O(2)	8(d)	0.285(4)	0.030(3)	−0.285(4)	0.3
$x = 0.4$	$a = 5.3682(2)$ Å	$b = 7.5699(3)$ Å	$c = 5.3503(2)$ Å		
	$R_{WP} = 12.84\%$	$R_p = 8.45\%$	$R_I = 2.95\%$		$R_F = 2.34\%$
Atom	Position	x	y	z	B
La, Ca	4(c)	0.027(1)	0.25	−0.008(2)	0.3
Mn, Ti	4(b)	0	0	0.5	0.3
O(1)	4(c)	0.486(3)	0.25	0.070(6)	0.3
O(2)	8(d)	0.285(3)	0.030(3)	−0.286(4)	0.3
$x = 0.6$	$a = 5.3994(5)$ Å	$b = 7.5984(7)$ Å	$c = 5.3742(4)$ Å		
	$R_{WP} = 15.17\%$	$R_p = 11.15\%$	$R_I = 3.79\%$		$R_F = 2.41\%$
Atom	Position	x	y	z	B
La, Ca	4(c)	0.027(1)	0.25	−0.009(2)	0.3
Mn, Tc	4(b)	0	0	0.5	0.3
O(1)	4(c)	0.488(4)	0.25	0.070(7)	0.3
O(2)	8(d)	0.280(5)	0.029(4)	−0.284(4)	0.3
$x = 0.8$	$a = 5.4371(2)$ Å	$b = 7.6462(3)$ Å	$c = 5.3969(2)$ Å		
	$R_{WP} = 10.33\%$	$R_p = 6.92\%$	$R_I = 2.61\%$		$R_F = 3.16\%$
Atom	Position	x	y	z	B
La, Ca	4(c)	0.030(1)	0.25	−0.006(1)	0.3
Mn, Ti	4(b)	0	0	0.5	0.3
O(1)	4(c)	0.486(2)	0.25	0.070(3)	0.3
O(2)	8(d)	0.288(2)	0.030(1)	−0.288(2)	0.3
$x = 0.9$	$a = 5.4527(1)$ Å	$b = 7.6570(2)$ Å	$c = 5.4060(1)$ Å		
	$R_{WP} = 10.82\%$	$R_p = 7.51\%$	$R_I = 3.28\%$		$R_F = 2.43\%$
Atom	Position	x	y	z	B
La, Ca	4(c)	0.031(1)	0.25	−0.007(1)	0.3
Mn, Ti	4(b)	0	0	0.5	0.3
O(1)	4(c)	0.486(2)	0.25	0.072(3)	0.3
O(2)	8(d)	0.286(1)	0.035(1)	−0.286(2)	0.3

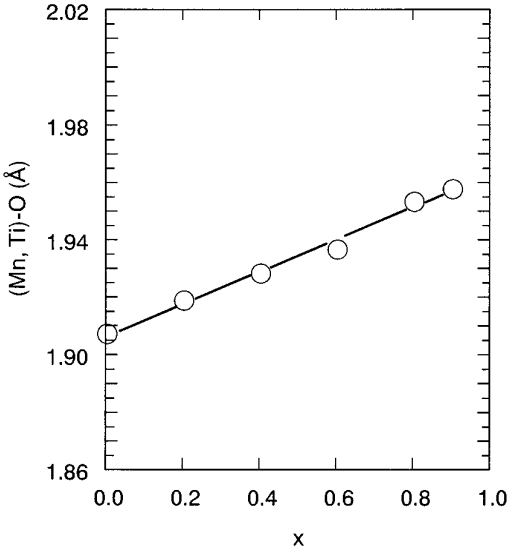

FIG 3. Average (Mn, Ti)–O distance vs composition (x) for the system $(La_{0.1}Ca_{0.9})(Mn_{1-x}Ti_x)O_3$.

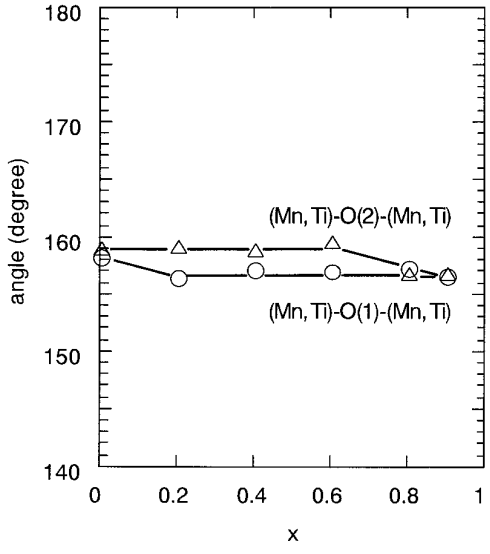

FIG 4. Angles for (Mn, Ti)–O(1)–(Mn, Ti) and (Mn, Ti)–O(2)–(Mn, Ti) vs composition (x) for the system $(La_{0.1}Ca_{0.9})(Mn_{1-x}Ti_x)O_3$.

at 0.3 Å for all samples (12). Refined structure parameters are summarized in Table 1. In Table 1, R_{WP}, R_P, R_I, and R_F are the weighted pattern, the pattern, the integrated intensity, and the structure factor, respectively. Final R_F of all samples was less than 3.33%. Therefore, the low R_F suggests that the structure model for $(La_{0.1}Ca_{0.9})(Mn_{1-x}Ti_x)O_3$ is good.

In the orthorhombic $GdFeO_3$-type structure, the La and Ca ions (A-site cations) coordinate with twelve anions; four O(1) and eight O(2) ions. The Mn and Ti ions (B-site cations) coordinate with six anions; two O(1) and four O(2) ions. Figure 3 shows the relationship between the average (Mn, Ti)–O distance of $(La_{0.1}Ca_{0.9})(Mn_{1-x}Ti_x)O_3$ calculated from the refined structural parameters and the composition. The average Mn–O distance of $(La_{0.1}Ca_{0.9})MnO_3$($x = 0$) is ca. 1.907 ± 0.010 Å. Because the ionic radius of the Ti^{4+} ion is larger than the ionic radii of the Mn^{4+} ion, the average (Mn, Ti)–O distance increases linearly with increasing x (10). The angles for O–(Mn, Ti)–O and (Mn, Ti)–O–(Mn, Ti) of $(La_{0.1}Ca_{0.9})(Mn_{1-x}Ti_x)O_3$ are calculated from the refined structural parameters. The average angles for O(1)–(Mn, Ti)–O(1), O(1)–(Mn, Ti)–O(2), and O(2)–(Mn, Ti)–O(2) are 180°, 90°, and 90° or 180°, respectively. From the results of the average (Mn, Ti)–O distances and the average angles for O–(Mn, Ti)–O, it is considered that each (Mn, Ti)O_6 octahedron has little distortion. The average angles for (Mn, Ti)–O(1)–(Mn, Ti) and (Mn, Ti)–O(2)–(Mn, Ti) are less than 180°, and are shown in Fig. 4. The average angles for both (Mn, Ti)–O(1)–(Mn, Ti) and (Mn, Ti)–O(2)–(Mn, Ti) decrease slightly with increasing x.

Figure 5 shows the relationship between the logarithm of the electrical resistivity (log ρ) of $(La_{0.1}Ca_{0.9})(Mn_{1-x}Ti_x)O_3$ and the reciprocal temperature (1000/T). At low temperature, all samples are n-type semiconductors, and log ρ increases abruptly with increasing x. The energy gap (E_g) calculated from the linear portion of the log ρ–1000/T curves is shown in Fig. 6. E_g of $x = 0.0$ is ca. 0.08 eV, and E_g has a constant value with ca. 0.15 ± 0.02 eV in the range $0.1 \leq x \leq 0.4$; then, E_g increases to ca 0.87 eV ($x = 0.9$).

The relation between the electrical resistivity (ρ) of $(La_{0.1}Ca_{0.9})(Mn_{1-x}Ti_x)O_3$ and temperature (T) in the range from 200 to 953 K is shown in Fig. 7. In the range $0.0 \leq$

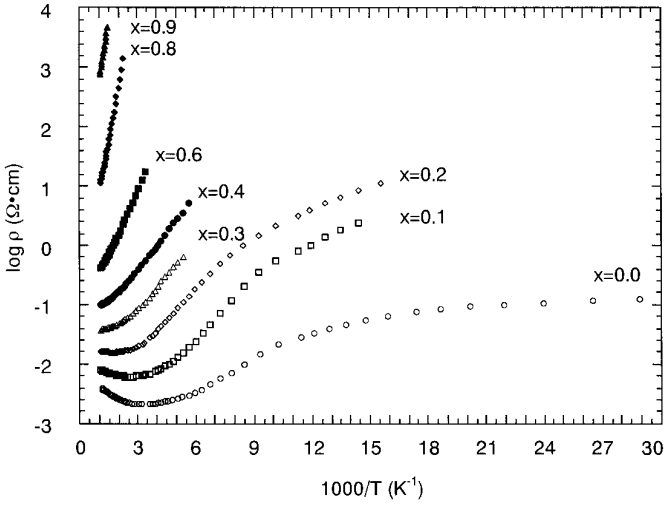

FIG 5. Logarithm electrical resistivity (log ρ) vs 1000/T for the system $(La_{0.1}Ca_{0.9})(Mn_{1-x}Ti_x)O_3$.

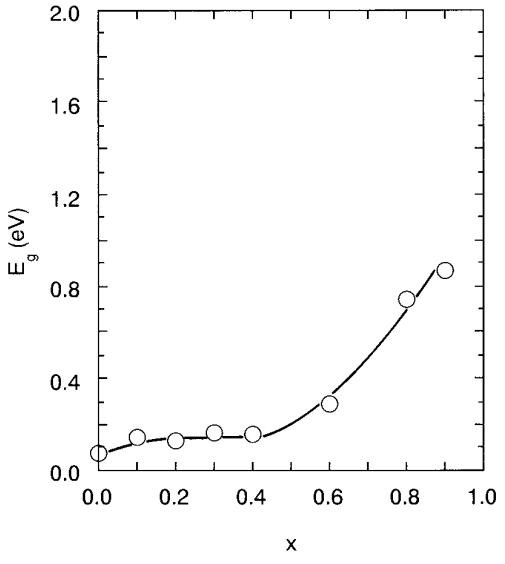

FIG 6. Energy gap (E_g) vs composition (x) for the system $(La_{0.1}Ca_{0.9})(Mn_{1-x}Ti_x)O_3$.

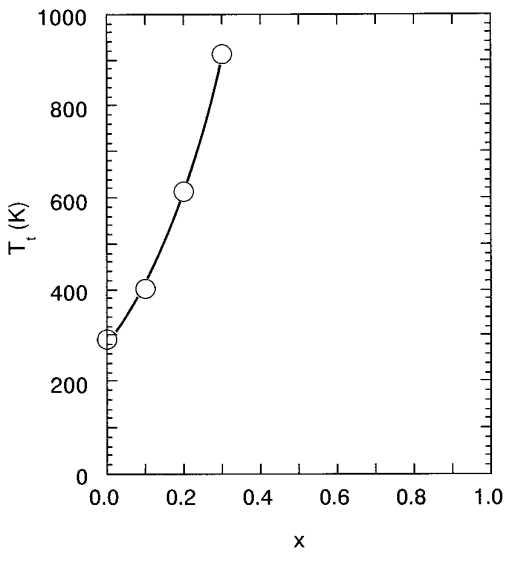

FIG 8. Metal-insulator transition temperature (T_t) vs composition (x) for the system $(La_{0.1}Ca_{0.9})(Mn_{1-x}Ti_x)O_3$.

$x \leq 0.3$, the electrical resistivity (ρ) has a positive temperature coefficient (α) at high temperature, and increases linearly with increasing temperature. From these results, it is obvious that $(La_{0.1}Ca_{0.9})(Mn_{1-x}Ti_x)O_3$ exhibits a metal–insulator transition. We defined the metal–insulator transition temperature (T_t) as the temperature where α changes from negative to positive. Figure 8 shows the relationship between T_t and composition. T_t of $x = 0.0$ is ca. 290 K, and increases monotonically to ca. 914 K ($x = 0.3$). ρ is generally given by

$$\rho = \rho_0 + \rho' \alpha T,$$

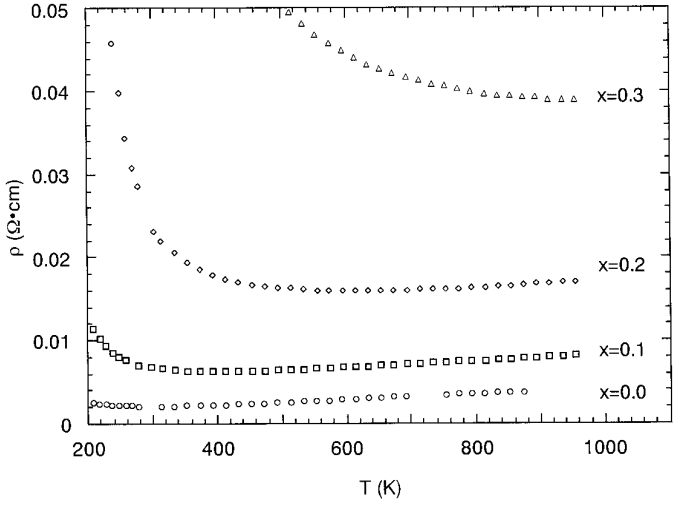

FIG 7. Electrical resistivity (ρ) vs temperature (T) for the system $(La_{0.1}Ca_{0.9})(Mn_{1-x}Ti_x)O_3$.

where ρ_0 is a constant depending on the impurity content, ρ' is a constant, α is a temperature coefficient, and T is temperature (8). As the sintered samples were used to measure the electrical resistivity, we used $d\rho/dT$ which is given by

$$d\rho/dT = \rho' \alpha,$$

because it is difficult to measure ρ' and α independently. $d\rho/dT$ values for $x = 0.0$, 0.1, and 0.2 are ca. 3.4×10^{-6}, 3.7×10^{-6}, and 4.0×10^{-6} $\Omega \cdot$ cm/K, respectively.

Taguchi and Shimada measured the differential thermal analysis (DTA) and the magnetic susceptibility (χ) of $(La_{1-x}Ca_x)MnO_3$ ($0.6 \leq x \leq 0.95$) (1). The samples gave neither exothermic nor endothermic peaks up to 1160 K. This result indicates that the samples exhibited the metal–insulator transition without any crystallographic change. A change in the slope of the $1/\chi$–T curve coincides with the metal–insulator transition, and the metal–insulator transition occurred by the change of the spin state of the Mn^{3+} ion. The $1/\chi$–T curve of $(La_{0.1}Ca_{0.9})(Mn_{0.8}Ti_{0.2})O_3$ ($x = 0.2$) is shown in Fig. 9. We can observe the deflection of the $1/\chi$–T curve at ca. 600 K. The effective magnetic moment (μ_{eff}) calculated from the $1/\chi$–T curve is ca. 3.20 μ_B in the range 403–593 K, and ca. 3.29 μ_B in the range 603–713 K, respectively. The increase of μ_{eff} suggests that there was a change of the spin state or the orbital character of the Mn ion. Goodenough proposed an energy band scheme for the perovskite type (13). The band scheme consists of the valence band (localized π^* orbital) and the conduction band (collective σ^* orbital) which are split by the electrostatic field (Δ). The localized π^* orbitals of α

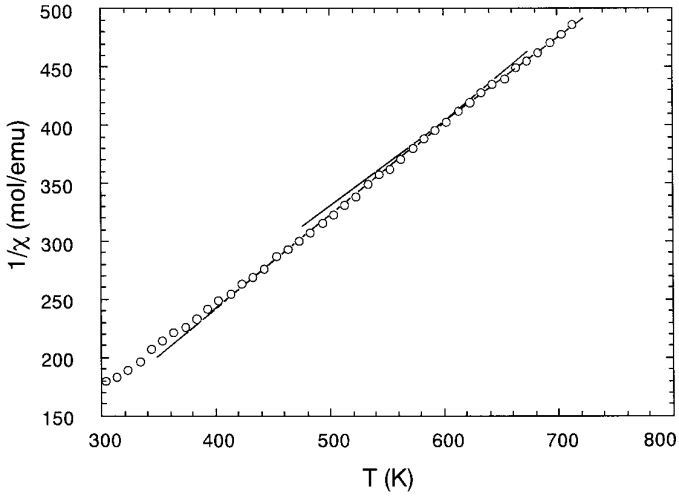

FIG 9. Inverse magnetic susceptibility ($1/\chi$) vs temperature (T) for $(La_{0.1}Ca_{0.9})(Mn_{0.8}Ti_{0.2})O_3$ ($x = 0.2$).

and β spins at a given cation are split by the intra-atomic exchange (E_{ex}), and collective π^* orbitals are likewise split by E_{ex}. We used this model to explain the mechanism of the metal–insulator transition in $(Ln_{1-x}Ca_x)MnO_3$. At low temperature, the $3d$ electrons exist in the localized π^*-α orbital. At high temperature, the increase of μ_{eff} suggests a change in the electronic state of the Mn ion. The $3d$ electrons coexist in the localized π^*-α orbital and the localized π^*-β orbital. In the case of $\Delta \leq E_{ex}$, the $3d$ electrons partially filled both the localized π^* orbitals and the collective σ^* orbitals, and $(Ln_{1-x}Ca_x)MnO_3$ exhibits metallic behavior. Therefore, it is considered that over three $3d$ electrons are necessary to exhibit the metal–insulator transition.

In the present $(La_{0.1}Ca_{0.9})(Mn_{1-x}Ti_x)O_3$ system, the number of $3d$ electrons of both Mn^{3+} and Ti^{4+} ions is independent of the composition. On the other hand, the number of the Mn^{4+} ions decreases linearly from 2.7 to 0.0. The total number of $3d$ electrons in $(La_{0.1}Ca_{0.9})(Mn_{1-x}Ti_x)O_3$ is 3.1–3.0x, and decreases with x. Since the total of $3d$ electrons of $(La_{0.1}Ca_{0.9})(Mn_{1-x}Ti_x)O_3$ is above 3.0 in the range $0.0 \leq x < 0.1$, the band model proposed by Goodenough is used to explain the metal–insulator transition. However, the total of $3d$ electrons of $(La_{0.1}Ca_{0.9})(Mn_{1-x}Ti_x)O_3$ is below 3.0 in the range $0.1 \leq x \leq 0.9$. In order to explain the mechanism of the metal–insulator transition for $(La_{0.1}Ca_{0.9})(Mn_{1-x}Ti_x)O_3$ ($0.1 \leq x \leq 0.9$), we propose the band model that the split (α and β spins) by the intra-atomic exchange (E_{ex}) disappeared in the range $0.1 \leq x \leq 0.9$. The $3d$ electrons exist in the localized π^* orbital at low temperature. With increasing temperature, the spin state of the Mn^{3+} ion changes partly low to high (Fig. 9), and the $3d$ electrons coexist in both the collective σ^* and the localized π^* orbitals. Therefore, $(La_{0.1}Ca_{0.9})(Mn_{1-x}Ti_x)O_3$ exhibits the metal–insulator transition. $d\rho/dT$ in the metallic region decreases with increasing x. The increase in $d\rho/dT$ is considered to be caused by the decrease in the number of $3d$ electrons in the collective σ^* orbital.

In the orthorhombic perovskite-type oxides, the (Mn, Ti)O_6 octahedron connects at O(1) or O(2) of the other's (Mn, Ti)O_6 octahedron, and there are two kinds of cation–anion–cation overlap; one is an overlap (π bond) between the cation $d\varepsilon^*$ and oxygen p_π orbitals, and the other is the overlap (σ bond) between the cation $d\gamma^*$ and oxygen p_σ orbitals (14). Below T_t, the cation–anion–cation overlap integrals (Δ^π_{cac} for π bond and Δ^σ_{cac} for σ bond) are smaller than the critical overlap integral (Δ_c); $\Delta^\pi_{cac} < \Delta^\sigma_{cac} < \Delta_c$. Above T_t, the cation–anion–cation overlap integrals are larger than the critical integral; $\Delta_c < \Delta^\pi_{cac} < \Delta^\sigma_{cac}$. If the average (Mn, Ti)–O distance and the number of $3d$ electrons are constant, a geometrical arrangement between the cation $d\gamma^*$ and oxygen p_σ orbitals indicates that σ bonding is stronger where the average angle for (Mn, Ti)–O(1)–(Mn, Ti) is 180°, and the decrease in the average angle for (Mn, Ti)–O(1)–(Mn, Ti) from 180° weakens σ bonding. On the other hand, the overlap between the cation $d\varepsilon^*$ and oxygen p_π orbitals increases with the deviation of the average angle for (Mn, Ti)–O(2)–(Mn, Ti) from 180°, that is, π bonding becomes stronger (12). Because the average angles for (Mn, Ti)–O–(Mn, Ti) decrease slightly with increasing x, both Δ^π_{cac} and Δ^σ_{cac} are not strongly affected by the angles for (Mn, Ti)–O–(Mn, Ti). Although E_g has a constant value with ca. 0.15 ± 0.02 eV, the average (Mn, Ti)–O distance increases and the number of $3d$ electrons decreases with increasing x. These variations make the electron density of the π^* orbital decrease, or make both Δ^π_{cac} and Δ^σ_{cac} weaken. Conseqeuntly, ρ, T_t, and E_{ex} of $(La_{0.1}Ca_{0.9})(Mn_{1-x}Ti_x)O_3$ are strongly influenced by the Ti^{4+} ion.

CONCLUSION

Rietveld analysis of $(La_{0.1}Ca_{0.9})(Mn_{1-x}Ti_x)O_3$ indicates that the average (Mn, Ti)–O distance increases linearly and the average angles for (Mn, Ti)–O–(Mn, Ti) decrease slightly with increasing x. $(La_{0.1}Ca_{0.9})(Mn_{1-x}Ti_x)O_3$ ($0 \leq x \leq 0.3$) exhibits the metal–insulator transition analogous to $(La_{1-x}Ca_x)MnO_3$. The compositional dependence of $d\rho/dT$ in the metallic region is caused by the decrease in the number of $3d$ electrons in the collective σ^* orbital. The Ti^{4+} ion in $(La_{0.1}Ca_{0.9})(Mn_{1-x}Ti_x)O_3$ makes the cation–anion–cation overlap integrals (Δ^π_{cac} and Δ^σ_{cac}) weaken.

ACKNOWLEDGMENT

The present work was supported by Grant-in-Aid for Scientific Research 06453078 from the Ministry of Education, Science and Culture of Japan, and by The Murata Science Foundation.

REFERENCES

1. H. Taguchi and M. Shimada, *J. Solid State Chem.* **63,** 290 (1986).
2. H. Taguchi, M. Nagao, and M. Shimada, *J. Solid State Chem.* **76,** 284 (1988).
3. H. Taguchi, M. Nagao, and M. Shimada, *J. Solid State Chem.* **82,** 8 (1989).
4. T. Kobayahi, H. Takizawa, T. Endo, T. Sato, M. Shimada, H. Taguchi, and M. Nagao, *J. Solid State Chem.* **92,** 116 (1991).
5. M. Ohtaki, H. Koga, T. Tokunaga, K. Eguchi, and H. Arai, *J. Solid State Chem.* **120,** 105 (1995).
6. N. F. Mott, *Adv. Phys.* **21,** 785 (1972).
7. H. Taguchi, M. Nagao, and M. Shimada, *J. Solid State Chem.* **97,** 476 (1992).
8. H. Taguchi and M. Nagao, *J. Solid State Chem.* **105,** 392 (1993).
9. F. Izumi, *Nippon Kesho Gakkaishi* **27,** 23 (1985). [in Japanese]
10. R. D. Shannon and C. T. Prewitt, *Acta Crystallogr. Sect. B* **25,** 925 (1969).
11. K. R. Poeppelmeier, M. E. Leonowicz, J. C. Scanlon, and W. B. Yelon, *J. Solid State Chem.* **45,** 71 (1982).
12. H. Taguchi, M. Nagao, and Y. Takeda, *J. Solid State Chem.* **114,** 236 (1995).
13. J. B. Goodenough, *J. Appl. Phys.* **37,** 1415 (1966).
14. J. B. Goodenough, *Czech. J. Phys. B* **17,** 304 (1967).